

PDF hosted at the Radboud Repository of the Radboud University Nijmegen

The following full text is a publisher's version.

For additional information about this publication click this link.

<http://hdl.handle.net/2066/168544>

Please be advised that this information was generated on 2019-06-19 and may be subject to change.

Nonquasiparticle states in the half-metallic ferromagnet NiMnSbL. Chioncel,¹ M. I. Katsnelson,^{1,2,3} R. A. de Groot,¹ and A. I. Lichtenstein¹¹*University of Nijmegen, NL-6525 ED Nijmegen, The Netherlands*²*Institute of Metal Physics, 620219 Ekaterinburg, Russia*³*Department of Physics, Uppsala University, Box 530, SE-75121 Uppsala, Sweden*

(Received 24 March 2003; revised manuscript received 27 August 2003; published 17 October 2003)

Nonquasiparticle states above the Fermi energy are studied by first-principle dynamical mean field calculations for a prototype half-metallic ferromagnet NiMnSb. We present a quantitative evaluation of the spectral weight of this characteristic feature and discuss the possible experimental investigation (Bremsstrahlung isohromat spectroscopy, nuclear magnetic resonance, scanning tunneling microscopy, and Andreev reflection) to clarify the existence of these states.

DOI: 10.1103/PhysRevB.68.144425

PACS number(s): 75.50.Cc, 71.10.-w, 71.20.Be

I. INTRODUCTION

Half-metallic ferromagnets (HMF's)¹⁻³ are now a subject of growing interest, first of all, because of their possible applications to “spintronics,” that is, spin-dependent electronics.⁴ Being metals for one spin projection and semiconductors for the opposite one¹ they have order-in-magnitude different spin contributions to electronic transport properties which can result in a huge magnetoresistance for heterostructures containing HMF's.² In addition to heterostructure systems, bulk materials such as $\text{La}_{1-x}\text{Sr}_x\text{MnO}_3$ (Ref. 5) compound, combining half-metallic ferromagnetism and colossal magnetoresistance, has also attracted more attention to this problem.

As a result, numerous first-principle electronic structure calculations of HMF's have been carried out, starting from Ref. 1 (see, e.g., recent papers^{6,7} and a review of early works in Ref. 2). All of them are based on a standard local density approximation (LDA) or generalized gradient approximation (GGA) of the density functional theory or, sometimes, on the LDA+U approximation (Ref. 8 for CrO_2). All of these approaches completely neglect the effects of dynamical spin fluctuations on the electronic structure which can be of crucial importance for HMF's.

The appearance of nonquasiparticle states in the energy gap near the Fermi level^{9,10} is one of the most interesting correlation effects typical for HMF's. The origin of these states is connected with “spin-polaron” processes: the spin-down low-energy electron excitations, which are forbidden for HMF's in the one-particle picture, turn out to be possible as superpositions of spin-up electron excitations and virtual magnons. The density of these nonquasiparticle states vanishes at the Fermi level but increases drastically at the energy scale of the order of a characteristic magnon frequency ω_m , giving an important contribution, in the temperature dependence of the conductivity due to the interference with impurity scattering.² It is worthwhile to mention that the existence of such a nonquasiparticle state is important for spin-polarized electron spectroscopy,^{10,11} NMR,¹² and subgap transport in ferromagnet-superconductor junctions (Andreev reflection).¹³

The temperature dependence of the HMF electronic structure and stability of half-metallicity against different spin

excitations are crucial for practical applications in spintronics. A simple attempt to incorporate the static noncollinear spin configurations, due to finite-temperature effects,¹⁴ shows the mixture of spin up and spin down density of states that destroy the half-metallic behavior. It is our scope to use a more natural many-body approach to investigate the proper dynamical spin fluctuations effect on the electronic structure at temperatures $T < T_c$, within the half-metallic ferromagnetic state.

In this paper we present the first quantitative theory of nonquasiparticle states in HMF based on realistic electronic structure calculation in NiMnSb. The combination of local density approximation in the frame of density functional theory with the many-body technique allowed us to estimate the spectral weight of the nonquasiparticle states. Various possibilities of experimental manifestations of such a states are discussed at the end of the paper.

**II. NONQUASIPARTICLE STATES:
AN ILLUSTRATIVE EXAMPLE**

Before the investigation of the real NiMnSb material it is worthwhile to illustrate the correlation effects on the electronic structures of HMF using a simple “toy” model. The one-band Hubbard model of a saturated ferromagnet can provide us the simplest model of a half-metallic state

$$H = - \sum_{i,j,\sigma} t_{ij} (c_{i\sigma}^\dagger c_{j\sigma} + c_{j\sigma}^\dagger c_{i\sigma}) + U \sum_i n_{i\uparrow} n_{i\downarrow}. \quad (1)$$

Difficulties in solving the Hubbard model Eq. (1) are well known.⁹ Fortunately there is an exact numerical solution in the limit of infinite dimensionality or large connectivity called dynamical mean field theory (DMFT).¹⁵ Following this approach we will consider the Bethe lattice with coordination $z \rightarrow \infty$ and nearest neighbor hopping $t_{ij} = t/\sqrt{z}$. In this case a semicircular density of states is obtained as function of the effective hopping t : $N(\epsilon) = (1/2\pi t^2) \sqrt{4t^2 - \epsilon^2}$. To stabilize the ferromagnetic solution within the Hubbard model is yet another difficult problem. It was proved recently, that the necessary conditions for ferromagnetism is a density of state with large spectral weight near the band edges¹⁶ and the Hund's rule coupling for the degenerate case.¹⁷ In our “toy”

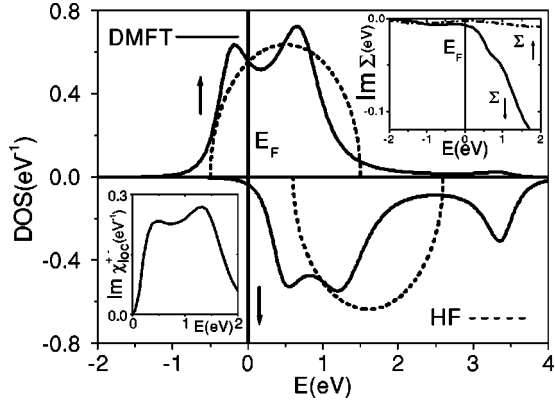


FIG. 1. Density of states for HMF in the Hartree-Fock (HF) approximation (dashed line) and the QMC solution of DMFT problem for the semicircular model (solid line) with the band width $W = 2$ eV, Coulomb interaction $U = 2$ eV, spin splitting $\Delta = 0.5$ eV, chemical potential $\mu = -1.5$ eV, and temperature $T = 0.25$ eV. Insets: imaginary part of the local spin-flip susceptibility (left) and the spin-resolved self-energy (right).

model in order to stabilize the HMF state, we add an external magnetic spin splitting term $\Delta = 0.5$ eV, which mimic the local Hund polarization originated from other orbitals in the real NiMnSb compound. This HMF state corresponds to a mean-field (HF) solution with a LSDA-like DOS, denoted in Fig. 1 as dashed line.

DMFT maps the many-body system, Eq. (1), onto the self-consistent quantum impurity model with the effective action.¹⁵

$$S_{\text{eff}} = - \int_0^\beta d\tau \int_0^\beta d\tau' c_\sigma^\dagger(\tau) \mathcal{G}_\sigma^{-1}(\tau - \tau') c_\sigma(\tau') + \int_0^\beta d\tau U n_\uparrow(\tau) n_\downarrow(\tau). \quad (2)$$

The effective medium Green function \mathcal{G}_σ (Weiss function) is connected with the local Green function G_σ through the self-consistency condition

$$\mathcal{G}_\sigma^{-1} = i\omega + \mu - t^2 G_\sigma - 1/2\sigma\Delta, \quad (3)$$

where $\omega = (2n+1)\pi T$, $n = 0, \pm 1, \pm 2, \dots$, represents the Matsubara frequencies corresponding to a temperature T and τ is the imaginary time. The Green function corresponding to the DMFT effective action (2): $\mathcal{G}_\sigma(\tau - \tau') = -\langle T_\tau c_\sigma(\tau) c_\sigma^\dagger(\tau') \rangle_{S_{\text{eff}}}$ have been calculated using the quantum Monte Carlo scheme within the so-called exact enumeration technique, with the number of time slices $L = 25$. T_τ represents the time ordering operator. We would like to emphasize that due to the symmetry of the ferromagnetic state the local G_σ and the effective medium \mathcal{G}_σ Green functions are diagonal in spin space, even in the presence of the interaction part of the effective action (2) which describes the spin-flip scattering process.

The applicability of the local approximation to the problem of existence of the nonquasiparticle states has been discussed in Ref. 18. In this limit it is possible to capture some

features of the magnetic excitations, namely those which can be described by the spin susceptibility $\chi(\mathbf{q}, i\omega)$ for $\mathbf{q} = 0$ and $\mathbf{q} = \pi$ (ferromagnetic and antiferromagnetic long-range order, correspondingly).¹⁹ As for the case of a generic \mathbf{q} it is worthwhile to stress that the accurate description of the magnon spectrum is not important for the existence of the nonquasiparticle states and for the proper estimation of their spectral weight, but can be important to describe an explicit shape of the density of states “tail” in a very close vicinity of the Fermi energy. The DMFT, being an optimal *local* approximation for the electron self-energy,¹⁵ should be adequate for the description of nonquasiparticle states, because of the weak momentum dependence of the corresponding contributions to the electron Green function.

Our model allows us to study the magnon spectrum through the two-particle correlation function which is obtained using the QMC procedure.¹⁹ We calculate the local spin-flip susceptibility

$$\chi_{\text{loc}}^{+-}(\tau - \tau') = \langle S^+(\tau) S^-(\tau') \rangle = \langle T_\tau c_\uparrow^\dagger(\tau) c_\downarrow(\tau) c_\downarrow^\dagger(\tau') c_\uparrow(\tau') \rangle_{S_{\text{eff}}} \quad (4)$$

which gives us information about the integrated magnon spectrum.^{10,20}

The DMFT results are presented in Fig. 1. In comparison with a simple Hartree-Fock solution one can see an additional well-pronounced feature appearing in the spin-down gap region, just above the Fermi level. This new many-body feature corresponds to the so-called nonquasiparticle states in HMF’s (Refs. 9,10) and represents the spin-polaron process:^{9,10} the spin-down electron excitations forbidden in the one electron description of HMF are possible due to the superposition of spin-up electron excitations and virtual magnons. In addition to this nonquasiparticle states visible in both spin channels of DOS around 0.5 eV, a many-body satellite appears at 3.5 eV.

The left inset of Fig. 1, represents the imaginary part of local spin-flip susceptibility. One can see a well pronounced shoulder (≈ 0.5 eV), which is related to a characteristic magnon excitation.¹⁰ In addition there is a broad maximum (≈ 1 eV) corresponding to the Stoner excitation energy. The right inset of Fig. 1, represents the imaginary part of self-energy calculated from our “toy model.” The spin up channel can be described by a Fermi-liquid-type behavior, with a parabolic energy dependence $-\text{Im} \Sigma^\uparrow \approx (E - E_F)^2$, where as in the spin down channel, of Σ^\downarrow , the nonquasiparticle shoulder at 0.5 eV, is visible. Due to the relatively high temperature ($T = 0.25$ eV) in our QMC calculation the nonquasiparticle tail goes below the Fermi level. At zero temperature ($T = 0$) the tail should end exactly at the Fermi level.¹⁰ Since the exact enumeration technique not “suffer” from the QMC noise, the Pade analytical continuation was used to extract spectral functions and density of states.²¹

The existence of the nonquasiparticle states for this model has been proven by perturbation-theory arguments⁹ (i.e., for a broad-band case) and in the opposite infinite- U limit.¹⁰ Physically, the appearance of these states can be considered as a kind of spin-polaron effect. According with the conser-

vation laws, in the many-body theory the spin-down state with the quasimomentum \mathbf{k} can form a superposition with the spin-up states with the quasimomentum $\mathbf{k} - \mathbf{q}$ plus a magnon with the quasimomentum \mathbf{q} , \mathbf{q} running the whole Brillouin zone. Taking into account the restrictions from the Pauli principle (an impossibility to scatter into occupied states) one can prove that this superposition can form only above the Fermi energy (here we consider the case where the spin-up electronic structure is metallic and the spin-down is semiconducting; oppositely, the nonquasiparticle states form only *below* the Fermi energy).^{2,10} If we neglect the magnon energy in comparison with the typical electron one than the density of nonquasiparticle states will vanish abruptly right at the Fermi energy; more accurate treatment shows that it vanishes continuously in the interval of the order of the magnon energy with a law which is dependent on the magnon dispersion.⁹ As a consequence the nonquasiparticle states are almost currentless.^{2,10} Recently, some evidences of the existence of almost currentless states near the Fermi energy in half-metallic ferromagnet CrO_2 have been obtained by x-ray spectroscopy.²²

III. COMPUTATIONAL METHOD

Recently, an approach to include correlation effects into the first-principle electronic structure calculations by the combination of the LDA with dynamical mean-field theory (DMFT) (for review of DMFT, see Ref. 15) has been proposed.^{23,24} In this case the DMFT maps a lattice many-body system onto multiorbital impurity model subject to a self-consistent condition in such a way that the many-body problem splits into one-body impurity problem for the crystal and the many-body problem for an effective atom. Therefore, the approach is complementary to the local (spin) density approximation,^{25–27} where the many-body problem splits into one-body problem for a crystal and many-body problem for *homogeneous* electron gas. Naively speaking, the LDA+DMFT method^{23,24} treats *d* and *f* electrons in spirit of DMFT and *s,p* electrons in spirit of LDA. Of course, this is a crude description since these two subsystems are not considered as independent ones but connected by the self-consistency conditions. In fact, the DMFT, due to numerical and analytical techniques developed to solve the effective impurity problem,¹⁵ is a very efficient and extensively used approximation for energy dependent self-energy $\Sigma(\omega)$. The emerged LDA+DMFT method can be used for calculating a large number of systems with different strength of the electronic correlations (for detailed description of the method and computational results, see Refs. 28–30). The LDA+DMFT method appeared to be efficient in the consideration of a series of classical problems which were beyond the standard density functional theory, for example, electronic structure of the Mott-Hubbard insulators,³¹ magnetism of transition metals at finite temperatures³² and α - δ transition in Pu.³³ Here we present the results of LDA+DMFT calculations of the electronic structure of a “prototype” half-metallic ferromagnet NiMnSb.

In order to integrate the dynamical mean field approach into the band structure calculation we use the so called exact

muffin-tin orbital method (EMTO).^{34,35} In our current implementation,³⁶ in addition to the usual self-consistency of the many-body problem (self-consistency of the self-energy), we also achieved charge self-consistency. In the EMTO approach the one electron effective potential is represented by the optimized overlapping muffin-tin potential,^{34,35} which is the best possible spherical approximation to the full one-electron potential. The effective potential is used to calculate the one-electron Green function $G_{\text{EMTO}}(\mathbf{k}, z)$, on an arbitrary complex energy contour z , which encloses the valence band poles of the one-electron Green function. For core electrons a frozen core approach is used. For any Bloch wave vector \mathbf{k} from the Brillouin zone and complex energy z , the local multiorbital self-energy $\Sigma(z)$ is added to the LDA Green function via the Dyson equation³⁶

$$G(z) = \sum_{\mathbf{k}} [G_{\text{EMTO}}^{-1}(\mathbf{k}, z) - \Sigma(z)]^{-1} \quad (5)$$

(all the quantities here are matrices in spin, orbital, and, for several atoms per unit cell, site indices). In the iteration procedure the LDA+DMFT Green function (5) is used to calculate the charge and spin densities. Finally, for the charge self-consistency calculation we construct the new LDA effective potential from the spin and charge densities,³⁶ using the Poisson equation in the spherical cell approximation.³⁷

For the interaction Hamiltonian, we have taken the most general rotationally invariant form of the generalized Hubbard (on-site) Hamiltonian.²⁴ The many-body problem is solved using the SPTF method proposed in Ref. 41, which is a development of the earlier approach.²⁴ The SPTF approximation is a multiband spin-polarized generalization of the fluctuation exchange approximation (FLEX) of Bickers and Scalapino, but with a different treatment of particle-hole (PH) and particle-particle (PP) channels. The particle-particle channel is described by a *T*-matrix approach³⁹ giving a renormalization of the effective interaction. This effective interaction is used explicitly in the particle-hole channel. Justifications, further developments and details of this scheme can be found in Ref. 41. Here we present the final expressions for the electron self-energy. The sum over the ladder graphs leads to the replacement of the bare electron-electron interaction by the *T* matrix which obeys the equation

$$\begin{aligned} \langle 13|T^{\sigma\sigma'}(i\Omega)|24\rangle &= \langle 13|v|24\rangle - T \sum_{\omega} \sum_{5678} \mathcal{G}_{56}^{\sigma}(i\omega) \\ &\times \mathcal{G}_{78}^{\sigma'}(i\Omega - i\omega) \langle 68|T^{\sigma\sigma'}(i\Omega)|24\rangle, \end{aligned} \quad (6)$$

where the matrix elements of the screened Coulomb interaction $\langle 13|v|24\rangle$ are expressed using the average Coulomb and exchange energies U, J .⁴¹ $|1\rangle = |j, m\rangle$, where (*j*) is the site number, (*m*) the orbital quantum number, σ, σ' are the spin indices, $T^{\sigma\sigma'}(i\Omega)$ represents the *T* matrix, and *T* is the temperature. In the following we write the perturbation expansion for the interaction (6). The two contributions to the self-energy are obtained by replacing of the bare interaction by a *T* matrix in the Hartree and Fock terms

$$\Sigma_{12}^{\sigma, \text{TH}}(i\omega) = T \sum_{\Omega} \sum_{34\sigma'} \langle 13 | T^{\sigma\sigma'}(i\Omega) | 24 \rangle \mathcal{G}_{43}^{\sigma'}(i\Omega - i\omega),$$

$$\Sigma_{12}^{\sigma, \text{TF}}(i\omega) = -T \sum_{\Omega} \sum_{34\sigma'} \langle 14 | T^{\sigma\sigma'}(i\Omega) | 32 \rangle \mathcal{G}_{34}^{\sigma'}(i\Omega - i\omega). \quad (7)$$

The four matrix elements of the bare longitudinal susceptibility represents the density-density (dd), density-magnetic (dm^0), magnetic-density (m^0d), and magnetic-magnetic channels (m^0m^0). The matrix elements couples longitudinal magnetic fluctuation with density magnetic fluctuation. In this case the particle-hole contribution to the self-energy is written in the Fourier transformed form

$$\Sigma_{12}^{\sigma, \text{PH}}(\tau) = \sum_{34\sigma'} W_{1342}^{\sigma\sigma'}(\tau) \mathcal{G}_{34}^{\sigma'}(\tau). \quad (8)$$

The particle-hole fluctuation potential matrix $W^{\sigma\sigma'}(i\omega)$ is defined in the FLEX approximation^{40,24} with the replacement of the bare interaction by the “static” T matrix. The effective particle-hole fluctuation potential is an energy dependent quantity and is determined self-consistently:

$$W^{\sigma\sigma'}(i\omega) = \begin{pmatrix} W_{\uparrow\uparrow}(i\omega) & W_{\uparrow\downarrow}(i\omega) \\ W_{\downarrow\uparrow}(i\omega) & W_{\downarrow\downarrow}(i\omega) \end{pmatrix}. \quad (9)$$

As can be seen from expression (9), the spin polarized T matrix FLEX approach describes the spin-flip scatterings corresponding to the nondiagonal part of the $W^{\sigma\sigma'}(i\omega)$ matrix.⁴¹ Nevertheless, the local and Weiss Green functions as well as the electronic self-energies are spin diagonal, due to the symmetry of the ferromagnetic state.

It is important to note that all of the above expressions for the self-energy, in the spirit of the DMFT approach, involve the Weiss Green function. The total self-energy is obtained from Eqs. (7) and (8):

$$\Sigma^{\sigma}(i\omega) = \Sigma^{\sigma, \text{TH}}(i\omega) + \Sigma^{\sigma, \text{TF}}(i\omega) + \Sigma^{\sigma, \text{PH}}(i\omega). \quad (10)$$

Since some part of the correlation effects are included already in the local spin-density approximation (LSDA) a “double counted” terms should be taken into account. To this aim, we start with the LSDA electronic structure and replace $\Sigma_{\sigma}(E)$ by $\Sigma_{\sigma}(E) - \Sigma_{\sigma}(0)$ in all equations of the LDA+DMFT method. It means that we only add *dynamical* correlation effects to the LSDA method.

We would like to emphasize that Eq. (8) includes spin flip scattering missing from the standard GW approach, and these processes are responsible for the appearance of spin-polaron, or nonquasiparticle, states in the energy gap of HMF. The T -matrix renormalization is important for proper description of these processes which can be demonstrated accurately for the Hubbard¹⁰ and s - d exchange⁴² models in the spin-wave temperature region; in both cases it is the T matrix (and not the bare interaction) that determines the amplitudes of electron-magnon interactions.

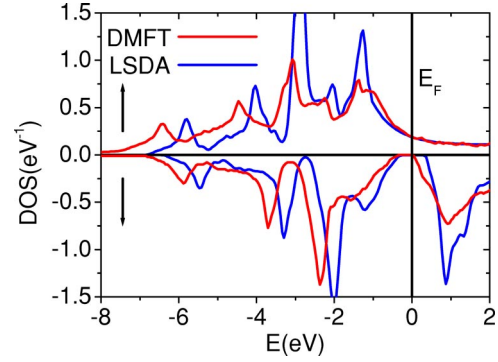


FIG. 2. Density of states for HMF NiMnSb in LSDA scheme (dashed line) and in LDA+DMFT scheme (solid line) with effective Coulomb interaction $U=3$ eV, exchange parameter $J=0.9$ eV, and temperature $T=300$ K. The nonquasiparticle state is evidenced just above the Fermi level.

IV. RESULTS: NiMnSb

In our LDA calculations we considered the standard representation of the $C1_b$ structure with a fcc unit cell containing three atoms Ni(0,0,0), Mn(1/4,1/4,1/4), Sb(3/4,3/4,3/4), and a vacant site $E(1/2,1/2,1/2)$, respectively. We used the experimental lattice constant of NiMnSb ($a=5.927$ Å) for all the calculations. To calculate the charge density we integrate along a contour on the complex energy plane which extends from the bottom of the band up to the Fermi level,³⁵ using 30 energy points. For Brillouin zone integration we sum up a k -space grid of 512 points in the irreducible part of the Brillouin zone. A cutoff of $l_{\text{max}}=8$ for the multipole expansion of the charge density and a cutoff of $l_{\text{max}}=3$ for the wave functions was used. The Perdew-Wang³⁸ parametrization of the local density approximation to the exchange correlation potential was used.

In order to incorporate the DMFT approach into the realistic electronic structure we need to evaluate the average on-site Coulomb repulsion energy U and the exchange interaction energy J . We used the constrained LDA calculation⁴³ which gives the value of the average Coulomb interaction between the Mn d electrons equal to $U=4.8$ eV and the exchange interaction energy equal to $J=0.9$ eV. Because the $3d$ orbitals of Ni are fully occupied, correlation effects are not so important. The insulating screening used in the constraint LDA calculation⁴³ should be generalized to a metallic one as in the case of HMF. Such a generalization will lead to additional reduction of the value of U . Therefore, we performed LDA+DMFT calculations for the different values of U between 0.5 and 4.8 eV. On the other hand, the results of constrained LDA calculations for the Hund exchange parameter J are not sensitive to the metallic screening.⁴⁴ Our LDA+DMFT results shows a very weak U dependence, due to the T -matrix renormalization.⁴¹ Figure 2 represents the typical results for density of states using the values of $U=3$ eV and $J=0.9$ eV. In comparison with the LDA the LDA+DMFT density of states shows the existence of new states in the LDA gap of the spin down channel just above the Fermi level.

It is important to mention that the magnetic moment per

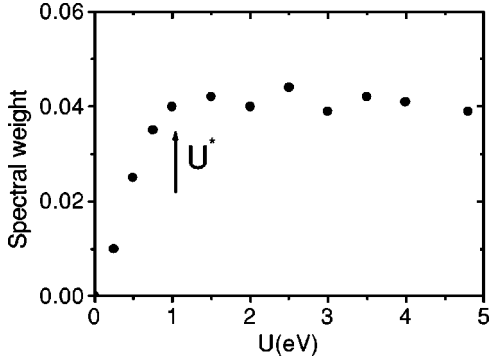


FIG. 3. Spectral weight of the nonquasiparticle state, calculated as function of average on-site Coulomb repulsion U at temperature $T=300$ K.

formula unit is not sensitive to the U values. For a temperature equal to $T=300$ K the calculated magnetic moment, $\mu = 3.96\mu_B$, is close to the integer LDA value $\mu = 4.00\mu_B$, which suggests that the half-metallic state is stable with respect to the introduction of the correlation effects. In addition, the DMFT gap in the spin down channel, defined as the distance between the occupied part and starting point of nonquasiparticle state's "tail," is also not very sensitive to the U values. For different U the slope of the "tail" is slightly changed, but the total DOS is weakly U dependent due to the T -matrix renormalization effects.

Thus the correlation effects do not effect too strongly on a general picture of the electron energy spectrum (except the smearing of the density of states features which is due to the finite temperature $T=300$ K in our calculations). The only qualitatively new effect is the appearance of the nonquasiparticle states in the energy gap above the Fermi energy. Their spectral weight for realistic values of the parameters are not too small which means that they should be well-pronounced in the corresponding experimental data. A relatively weak dependence of the nonquasiparticle spectral weight on the U value (Fig. 3) is also a consequence of the T -matrix renormalization.⁴¹

One can see that the T matrix is slightly dependent on U provided that the latter is larger than the widths of the main density of states peaks situated near the Fermi level (which is of the order of $U^* \approx 1$ eV) in an energy range of 2 eV.

For spin-up states we have a normal Fermi-liquid behavior $-\text{Im}\Sigma_d^\uparrow(E) \propto (E-E_F)^2$, with a typical energy scale of the order of several eV. The spin-down self-energy behaves in a similar way below the Fermi energy, with a bit smaller energy scale (which is still larger than 1 eV). At the same time, a significant increase in $\text{Im}\Sigma_d^\downarrow(E)$ with much smaller energy scale (tenths of eV) is evidenced right above the Fermi level which is more pronounced for t_{2g} states (Fig. 4). The nonquasiparticle states are visible in the spin \downarrow DOS Fig. 2, as well as in the spin \downarrow channel of the imaginary part of Σ_d^\downarrow , at the same energy. The similar behavior is evidenced in the model calculation Fig. 1.

According to the model consideration^{2,9,10} the width of this "jump" should be of the order of characteristic magnon energy which is much smaller than a typical electron band energy scale. In the simplest case of neglecting the disper-

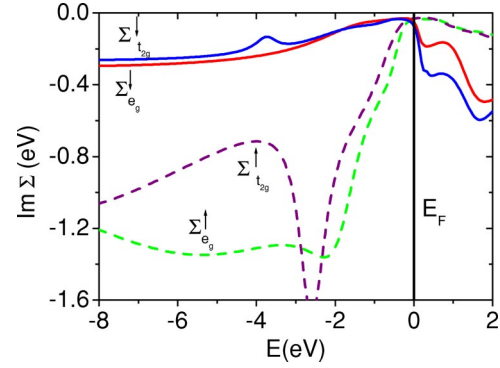


FIG. 4. The imaginary part of self-energies $\text{Im}\Sigma_d^\uparrow$ for t_{2g} (solid line) and e_g (dotted line) and $\text{Im}\Sigma_d^\downarrow$ for t_{2g} (dashed line) and e_g (dashed dotted line), respectively.

sion of the magnon frequency $\omega_{\mathbf{k}} \approx \omega_{\mathbf{m}}$ with respect to the electron hopping energy $t_{\mathbf{k}}$ the electronic self-energy becomes local:⁹

$$\begin{aligned} \Sigma_{\mathbf{k},\downarrow}(E) &= \frac{U^2 m}{N} \sum_{\mathbf{k}'} \frac{1-f(\mathbf{k}'\uparrow)}{E-t_{\mathbf{k}'\uparrow}+\omega_{\mathbf{k}-\mathbf{k}'}+i\delta} \\ &\approx \frac{U^2 m}{N} \sum_{\mathbf{k}'} \frac{1-f(\mathbf{k}'\uparrow)}{E-t_{\mathbf{k}'\uparrow}+\omega_{\mathbf{m}}+i\delta} = \Sigma_{\downarrow}^{\text{loc}}(E), \end{aligned}$$

where $f(\mathbf{k}'\sigma)$ is the Fermi distribution function. Therefore our main results (i) the existence of the nonquasiparticle states in real electronic structure of a specific compound and (ii) estimation of their spectral weight, can be obtained in the local LDA+DMFT approximation. The nonquasiparticle peak in the density of states (Fig. 2) is proportional to the imaginary part of the self-energy (Fig. 4), therefore it is determined by the processes of quasiparticle decay, which justifies the term "nonquasiparticle."

V. DISCUSSION AND CONCLUSIONS

From the point of view of the many-body theory, the general approach in the DMFT is to neglect the momentum dependence in the electron self-energy. In many cases such as the Kondo effect, the Mott metal-insulator transition, etc., the energy dependence of the self-energy is obviously much more important than the momentum dependence and, therefore, the DMFT is adequate to consider these problems.¹⁵ As for itinerant electron ferromagnetism, the situation is not completely clear. Note, however, that the LDA+DMFT treatment of finite temperature magnetism and electronic structure in Fe and Ni appeared to be quite successful.³² Experimentally, even in itinerant electron paramagnets close to ferromagnetic instability, such as Pd, the momentum dependence of the self-energy does not look to be essential.⁴⁵ One can expect that in magnets with well defined local magnetic moments such as half-metallic ferromagnets local approximation for the self-energy (i.e., the DMFT) should be even more accurate. In particular, as we discussed above, it can be used for the calculations of spin-polaronic (nonquasiparticle) effects in these materials.

Several experiments could be performed in order to clarify the impact of these nonquasiparticle states on spintronics. Direct ways of observing the nonquasiparticle states would imply the technique of Bremsstrahlung isochromat spectroscopy (BIS) (Ref. 46) or spin-polarized scanning tunneling microscopy.⁴⁷ In contrast with the photoelectron spectroscopy (spectroscopy of the occupied states) which show a complete spin polarization in HMF,⁵ BIS spectra should demonstrate an essential depolarization of the states above E_F , on the other hand SP-STM should also be able to probe these states which give the minority-spin contribution to the differential tunneling conductivity dI/dV .^{48,49} Another way to observe the nonquasiparticle states is the low-temperature measurement of the longitudinal nuclear magnetic relaxation rate $1/T_1$. Since the Korringa contribution due to the Fermi contact hyperfine interaction $1/T_1 \propto TN_{\downarrow}(E_F)N_{\uparrow}(E_F)$ vanishes for HMF a specific dependence, $1/T_1 \propto T^{5/2}$ (Ref. 10) should take place.⁵⁰ Andreev reflection spectroscopy using the tunneling junction superconductor—HFM (Ref. 13) can also be used in searching the experimental evidence of the nonquasiparticle states. Finally, we mention the spin-polarized STM techniques as a possible method of direct observation of the nonquasiparticle state in half-metallic fer-

romagnets. The spin-polarized scanning tunneling spectroscopy with positive bias voltage can in principle detect the opposite-spin state just above the Fermi level for surface of HMF such as CrO_2 . This experimental measurements will be of crucial importance for the theory of spintronics in any tunneling devices with half-metallic ferromagnets. In particular, I - V characteristics of half-metallic tunnel junctions for the case of antiparallel spins are completely determined by the nonquasiparticle states.⁵¹ Keeping in mind that ferromagnetic semiconductors can be considered as a peculiar case of HFM,² an account of these states can be important for proper description of spin diodes and transistors.^{52,13} Thus, the realistic computation of the spectral weight of nonquasiparticle states can be an interesting and important application of the LDA+DMFT approach.

ACKNOWLEDGMENTS

This work was supported by the Stichting for Fundamenteel Onderzoek der Materie (FOM-NWO), Nederlandse Organisatie voor Wetenschappelijk Onderzoek (NWO) Project No. 047-008-16. The authors thank to G.A. de Weijts, L. Vitos, I. A. Abrikosov, and O. Eriksson for fruitful discussions.

-
- ¹R.A. de Groot, F.M. Mueller, P.G. van Engen, and K.H.J. Buschow, *Phys. Rev. Lett.* **50**, 2024 (1983).
- ²V.Yu. Irkhin and M.I. Katsnelson, *Phys. Usp.* **37**, 659 (1994); *J. Phys.: Condens. Matter* **2**, 7151 (1990).
- ³W.E. Pickett and J. Moodera, *Phys. Today* **54**, 39 (2001).
- ⁴G.A. Prinz, *Science* **282**, 1660 (1998).
- ⁵J.H. Park, E. Vescovo, H.J. Kim, C. Kwon, R. Ramesh, and T. Venkatesan, *Nature (London)* **392**, 794 (1998).
- ⁶G.A. de Wijs and R.A. de Groot, *Phys. Rev. B* **64**, 020402 (2001).
- ⁷T. Shishidou, A.J. Freeman, and R. Asahi, *Phys. Rev. B* **64**, 180401 (2001).
- ⁸M.A. Korotin, V.I. Anisimov, D.I. Khomskii, and G.A. Sawatzky, *Phys. Rev. Lett.* **80**, 4305 (1998).
- ⁹D.M. Edwards and J.A. Hertz, *J. Phys. F: Met. Phys.* **3**, 2191 (1973).
- ¹⁰V.Yu. Irkhin and M.I. Katsnelson, *Fiz. Tverd. Tela (S.-Peterburg)* **25**, 3383 (1983) [*Sov. Phys. Solid State* **25**, 1947 (1983)]; *J. Phys. C* **18**, 4173 (1985); *J. Phys.: Condens. Matter* **2**, 7151 (1990).
- ¹¹M.I. Katsnelson and D.M. Edwards, *J. Phys.: Condens. Matter* **4**, 3289 (1992).
- ¹²V.Yu. Irkhin and M.I. Katsnelson, *Eur. Phys. J. B* **19**, 401 (2001).
- ¹³G. Tkachov, E. McCann, and V.I. Fal'ko, *Phys. Rev. B* **65**, 024519 (2001).
- ¹⁴R. Skomski and P.A. Dowben, *Europhys. Lett.* **58**, 544 (2002).
- ¹⁵A. Georges, G. Kotliar, W. Krauth, and M. Rozenberg, *Rev. Mod. Phys.* **68**, 13 (1996).
- ¹⁶M. Ulmke, *Eur. Phys. J. B* **1**, 301 (1998).
- ¹⁷D. Vollhardt, N. Blumer, K. Held and M. Kollar, *Advances In Solid State Physics* (Vieweg, Wiesbaden, 1999), Vol. 38, p. 383.
- ¹⁸A.V. Zarubin and V.Yu. Irkhin, *Phys. Solid State* **41**, 963 (1999).
- ¹⁹M. Jarrell, *Phys. Rev. Lett.* **69**, 168 (1992).
- ²⁰T. Moriya, *Spin Fluctuations in Itinerant Electron Magnetism* (Springer, Berlin, 1985), p. 239.
- ²¹H.J. Vidberg and J.W. Serene, *J. Low Temp. Phys.* **29**, 179 (1977).
- ²²E.Z. Kurmaev, A. Moewes, S.M. Butorin, M.I. Katsnelson, L.D. Finkelstein, J. Nordgren, and P.M. Tedrow, *Phys. Rev. B* **67**, 155105 (2003).
- ²³V.I. Anisimov, A.I. Poteryaev, M.A. Korotin, A.O. Anokhin, and G. Kotliar, *J. Phys.: Condens. Matter* **9**, 7359 (1997).
- ²⁴A.I. Lichtenstein and M.I. Katsnelson, *Phys. Rev. B* **57**, 6884 (1998); M.I. Katsnelson and A.I. Lichtenstein, *J. Phys.: Condens. Matter* **11**, 1037 (1999).
- ²⁵P. Hohenberg and W. Kohn, *Phys. Rev.* **136**, B864 (1964).
- ²⁶W. Kohn and L.J. Sham, *Phys. Rev.* **140**, A1133 (1965).
- ²⁷U. von Barth and L. Hedin, *J. Phys. C* **5**, 1629 (1972).
- ²⁸A. I. Lichtenstein and M. I. Katsnelson, in *Band Ferromagnetism. Ground State and Finite-Temperature Phenomena*, edited by K. Barbeschke, M. Donath, and W. Nolting, *Lecture Notes in Physics* (Springer-Verlag, Berlin, 2001); A. I. Lichtenstein, M. I. Katsnelson, and G. Kotliar, in *Electron Correlations and Materials Properties 2*, edited by A. Gonis, N. Kioussis, and M. Ciftan (Kluwer Academic/Plenum Publishers, Dordrecht, 2002).
- ²⁹K. Held, I. A. Nekrasov, G. Keller, V. Eyert, N. Bluemer, A. K. McMahan, R. T. Scalettar, T. Pruschke, V. I. Anisimov, and D. Vollhardt, in *Quantum Simulations of Complex Many-Body Systems: From Theory to Algorithms*, edited by J. Grotendorst, D. Marx, and A. Muramatsu, Vol. 10 of *NIC Series* (NIC, Juelich, 2002), p. 175.
- ³⁰G. Kotliar and S. Y. Savrasov, in *New Theoretical Approaches to Strongly Correlated Systems*, edited by A. M. Tselik (Kluwer, Dordrecht, 2001).
- ³¹K. Held, L.A. Nekrasov, N. Blumer, V.I. Anisimov, and D. Voll-

- hardt, *Int. J. Mod. Phys. B* **15**, 2611 (2001).
- ³²A.I. Lichtenstein, M.I. Katsnelson, and G. Kotliar, *Phys. Rev. Lett.* **87**, 067205 (2001).
- ³³S.Y. Savrasov, G. Kotliar, and E. Abrahams, *Nature (London)* **410**, 793 (2001).
- ³⁴O.K. Andersen, O. Jepsen, and G. Krier, in *Lectures on Methods of Electronic Structure Calculations*, edited by V. Kumar, O.K. Andersen, and A.Mookerjee (World Scientific Publishing, Singapore, 1994), p. 63; O.K. Andersen and T. Saha-Dasgupta, *Phys. Rev. B* **62**, R16 219 (2000).
- ³⁵L. Vitos, H.L. Skriver, B. Johansson, and J. Kollár, *Comput. Mater. Sci.* **18**, 24 (2000).
- ³⁶L. Chioncel, L. Vitos, I.A. Abrikosov, J. Kollár, M.I. Katsnelson, and A.I. Lichtenstein, *Phys. Rev. B* **67**, 235106 (2003).
- ³⁷L. Vitos, *Phys. Rev. B* **64**, 014107 (2001).
- ³⁸J.P. Perdew and Y. Wang, *Phys. Rev. B* **45**, 13 244 (1992).
- ³⁹V.M. Galitski, *Zh. Eksp. Teor. Fiz.* **34**, 115, 1011 (1958); J. Kanamori, *Prog. Theor. Phys.* **30**, 275 (1963).
- ⁴⁰N.E. Bickers and D.J. Scalapino, *Ann. Phys. (N.Y.)* **193**, 206 (1989).
- ⁴¹M.I. Katsnelson and A.I. Lichtenstein, *Eur. Phys. J. B* **30**, 9 (2002).
- ⁴²V.Yu. Irkhin and M.I. Katsnelson, *Sov. Phys. JETP* **61**, 306 (1985).
- ⁴³V.I. Anisimov and O. Gunnarsson, *Phys. Rev. B* **43**, 7570 (1991).
- ⁴⁴V.I. Anisimov, F. Aryasetiawan, and A.I. Lichtenstein, *J. Phys.: Condens. Matter* **9**, 767 (1997).
- ⁴⁵W. Joss, L.N. Hall, G.W. Crabtree, and J.J. Vuillemin, *Phys. Rev. B* **30**, 5637 (1984); J. Appel and D. Fay *ibid.* **30**, 6689 (1984).
- ⁴⁶J. Unguris, A. Seiler, R.J. Celotta, D.T. Pierce, P.D. Johnson, and N.V. Smith, *Phys. Rev. Lett.* **49**, 1047 (1982).
- ⁴⁷R. Wiesendanger, H.-J. Guntherodt, G. Guntherodt, R.J. Gambino, and R. Ruf, *Phys. Rev. Lett.* **65**, 247 (1990).
- ⁴⁸G. D. Mahan, *Many-Particle Physics* (Plenum Press, New York, 1990), Sec. 9.3.
- ⁴⁹Y. Meir and N.S. Wingreen, *Phys. Rev. Lett.* **68**, 2512 (1992).
- ⁵⁰Note that weaker dipole-dipole interactions result in a “residual” linear-in- T relaxation term but, nevertheless, the nonquasiparticle contribution $T^{5/2}$ should be easily observable; for details, see Ref. 12.
- ⁵¹V.Yu. Irkhin and M.I. Katsnelson, *Eur. Phys. J. B* **30**, 481 (2002).
- ⁵²M.E. Flatte and G. Vignale, *Appl. Phys. Lett.* **78**, 1273 (2001).